A Numerical Investigation of the Structural Performance of Two Types of Reinforced Concrete Two-Way Slabs

Joseph
Department of Architecture, Faculty of Engineering, Hasanuddin University, Makassar, Indonesia
yahazielazaryapurek@gmail.com

Nasruddin
Department of Architecture, Faculty of Engineering, Hasanuddin University, Makassar, Indonesia
nasruddin@unhas.ac.id (corresponding author)

Hartawan
Department of Architecture, Faculty of Engineering, Hasanuddin University, Makassar, Indonesia
hartawan@unhas.ac.id

Received: 27 July 2025 | Revised: 22 September 2025, 20 October 2025, and 7 November 2025 | Accepted: 15 November 2025

 DOI: https://doi.org/10.48084/etasr.13682

ABSTRACT

This study compares the flexural behavior of two Reinforced Concrete (RC) floor systems, the flat slab system and the beam-slab system, using Finite Element Modeling (FEM) in ABAQUS. Both models were designed with equal concrete volume and reinforcement weight to ensure a fair basis for comparison. The flat slab system showed broadly distributed cracking and lower stress concentrations but exhibited a lower flexural capacity, failing at a maximum load of 199.71 kN. In contrast, the beam-slab system developed more concentrated cracking near supports, experienced higher reinforcement stresses, and sustained a higher load of 213.53 kN, although with greater deflection. These results align with previous studies, indicating that the beam-slab system offers better crack control and load-bearing capacity, despite increased deformation. With identical material quantities, the beam-slab system demonstrated higher flexural stiffness, whereas the flat slab system offered greater architectural flexibility. Overall, the findings underscore important structural and practical considerations for selecting efficient and reliable floor systems in modern RC design.

Keywords-flat slab system; beam-slab system; finite element method; flexural behavior; reinforced concrete

I. INTRODUCTION

Floor systems are among the most critical components of RC buildings, as they strongly influence structural performance, cost efficiency, and architectural flexibility [1-3]. The two most common systems are the flat slab and the beam-slab, each offering distinct structural and architectural characteristics [4-6]. In a beam-slab system, beams are placed between columns to improve load transfer, stiffness, and flexural strength, while the flat slab system carries loads directly to the columns, providing greater architectural freedom by eliminating beams [7-9]. Advancements in structural engineering highlight the importance of Finite Element Analysis (FEA) for understanding the nonlinear behavior of RC slabs [10, 11]. FEM enables more accurate predictions of stress distribution, deflection, and crack development compared with traditional analytical approaches [12-14]. Previous studies report that flat slabs, although advantageous for rapid construction and open-space layouts, are more vulnerable to punching shear due to the lack of supporting beams [15, 16]. In contrast, beam-slab systems typically offer greater shear resistance and stiffness but require additional formwork, reinforcement, and construction effort [17-19]. Comparative research on two-way RC slabs further demonstrates that reinforcement detailing, load distribution, and span-to-depth ratios play key roles in determining flexural performance [20, 21]. Parametric studies also show that using lightweight concrete or high-performance materials can enhance structural efficiency by reducing self-weight without compromising safety [22-24]. Additionally, both experimental and numerical findings emphasize that reinforcement layout significantly affects crack propagation, ductility, and serviceability [25-27].

Strengthening strategies using Fiber-Reinforced Polymers (FRP) have been extensively explored to enhance the flexural capacity of both flat and beam-slab systems [28-30]. Finite element simulations demonstrate that FRP retrofitting increases

load-carrying capacity, delays crack formation, and improves overall ductility [31, 32]. Other studies have examined the punching shear resistance of flat slabs reinforced with shear studs, confirming the effectiveness of these elements in mitigating brittle failure mechanisms [33, 34]. Sustainability and material efficiency have also become key considerations in modern slab system design. FEM-based assessments of two-way concrete slabs have demonstrated that optimized reinforcement and slab thickness configurations can reduce both cost and environmental impact [35, 36]. Additionally, research into the stiffness, vibration, and strength of lightweight concrete flat slabs indicates that innovative materials can contribute to sustainable, low-carbon construction practices [37-39]. Despite these advancements, comprehensive comparative investigations between flat slab and beam-slab systems under identical material properties and loading conditions remain limited [40]. The behavior of either flat slabs or beam-slab systems using the FEM has been examined [27, 37]; however, few studies have conducted direct numerical comparisons considering equivalent material, geometric, and reinforcement parameters. To address this gap, the present study conducts a numerical comparison of flat slab and beam-slab systems using ABAQUS software, ensuring equivalent concrete volume and reinforcement weight for both configurations. The findings are expected to provide valuable insights for structural engineers in selecting the most efficient, economical, and sustainable floor system for RC buildings.

II. METHODOLOGY

This research adopts a numerical simulation approach using the FEM, implemented through ABAQUS software [19], a widely recognized tool in nonlinear structural analysis. The study aims to evaluate and compare the flexural behavior of two RC floor systems: flat slab and beam-slab, under similar material and load conditions to isolate the effect of structural configuration.

A. Model Configuration

The geometric and reinforcement details of both slab systems are illustrated in Figures 1 and 2. Both floor systems were designed in accordance with [17] to ensure a fair structural comparison by maintaining identical total concrete volume (0.51 m³) and reinforcement weight (57.44 kg). This approach eliminates the influence of material quantity differences, allowing the analysis to focus solely on the structural configuration. In the beam-slab system, as shown in Figure 1, the slab thickness was set to 120 mm, supported by beams with cross-sectional dimensions of 100 mm × 200 mm. The load was applied through a 700 mm × 700 mm steel plate positioned at the center of the slab to simulate realistic floor loading conditions. The slab was reinforced with Ø10 mm bars placed at 150 mm and 200 mm spacing in both directions on the top and bottom layers, while the beams contained 2Ø10 mm longitudinal bars at both the top and bottom and Ø8 mm stirrups spaced at 200 mm.

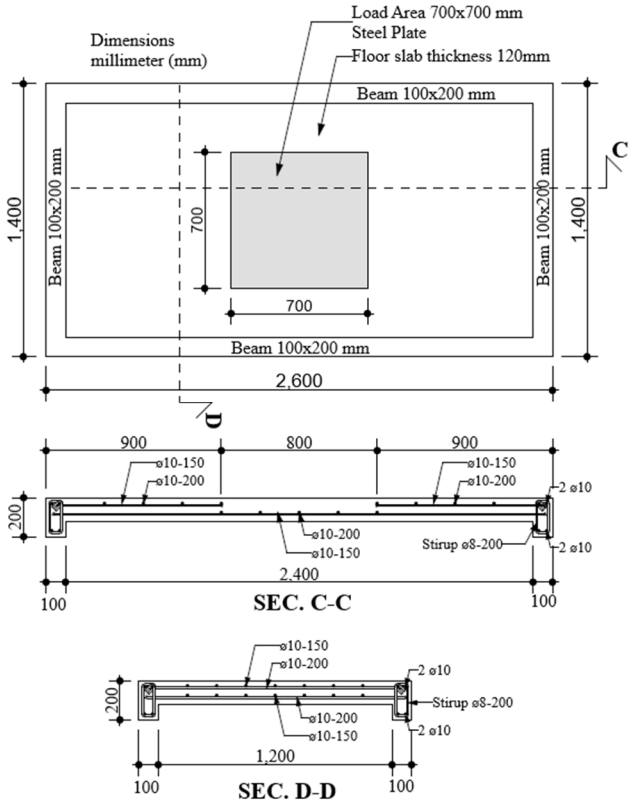

Fig. 1. Model of beam-slab system.

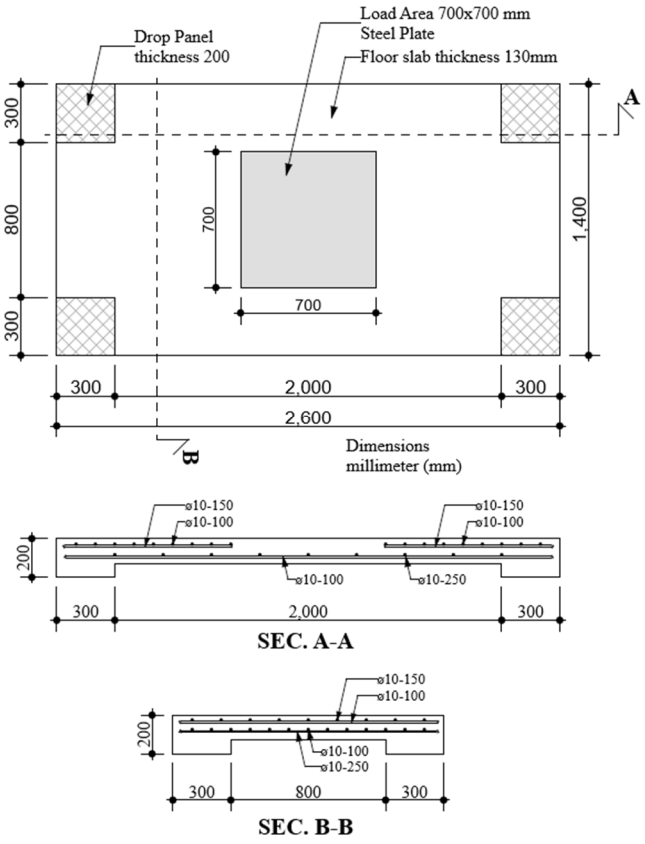

Fig. 2. Model of flat slab system.

In the flat slab system, as depicted in Figure 2, the slab thickness was modeled as 130 mm, with an additional 200 mm-thick drop panel located around the column region to enhance punching shear resistance. The slab contributed a volume of 0.43 m³, while the drop panel accounted for 0.08 m³, resulting in a total equal to the beam-slab model. The reinforcement consisted of Ø10 mm bars arranged at 100 mm, 150 mm, 200 mm, and 250 mm spacing in both directions and layers, with additional 2Ø10 mm bars provided in the column strip zones to improve flexural capacity. This configuration ensured that both systems utilized the same quantity of concrete and reinforcement while faithfully reflecting their respective structural layouts.

B. Material Properties

The material properties were: concrete compressive strength (f'_c): 25 MPa, reinforcing steel yield strength (f_y): 493 MPa, ultimate tensile strength (f_u): 750 MPa. Concrete was modeled using solid 3D elements (C3D8R) to capture nonlinear cracking behavior, while reinforcement bars were embedded using truss elements (T3D2) with the assumption of perfect bond.

C. Loading and Boundary Conditions

A concentrated load was applied through a 70 cm × 70 cm steel plate located at the center of the slab to replicate realistic distributed loads, such as equipment or point loads from occupancy. The boundary conditions simulate column support behavior by restraining translation at support points, allowing rotation to simulate pin conditions. The load was applied incrementally in a nonlinear static analysis until failure criteria were reached—either via convergence error or by attaining 90% concrete damage, as indicated by Abaqus' damage plasticity model.

D. Meshing and Convergence

A mesh convergence study was conducted to determine the appropriate element size that provides accurate results while maintaining computational efficiency. Four different element sizes were tested: 50 mm, 35 mm, 25 mm, and 15 mm. The corresponding ultimate loads obtained from the analysis were 195.2 kN, 198.5 kN, 199.7 kN, and 200.1 kN, respectively. As shown in Figure 3, the ultimate load increases with mesh refinement, but the difference between the 25 mm and 15 mm element sizes is less than 3%. This indicates that further mesh refinement beyond 25 mm provides only marginal improvements in accuracy, while significantly increasing the computational time. Therefore, an element size of 25 mm was selected as optimal, as it provides stable and reliable results with an acceptable balance between accuracy and efficiency. Both the slab and beams were modeled using this mesh density. Additionally, reduced integration and hourglass control were applied to ensure stability and to prevent numerical locking.

In this study, the ABAQUS models were developed using 12 mm reinforcement bars spaced at 150 mm, with C3D8R elements assigned to the concrete and T3D2 elements used for the reinforcement. A mesh size of 25 mm was selected based on mesh convergence analysis. The Concrete Damaged Plasticity (CDP) parameters, a dilation angle of 36°, an fb0/fc0 ratio of 1.16, and a Kc value of 0.667, were calibrated using published experimental data. Boundary conditions were applied at the column supports, and a uniformly distributed load was incrementally increased until structural failure. These modeling details ensure both the accuracy and reproducibility of the numerical results.

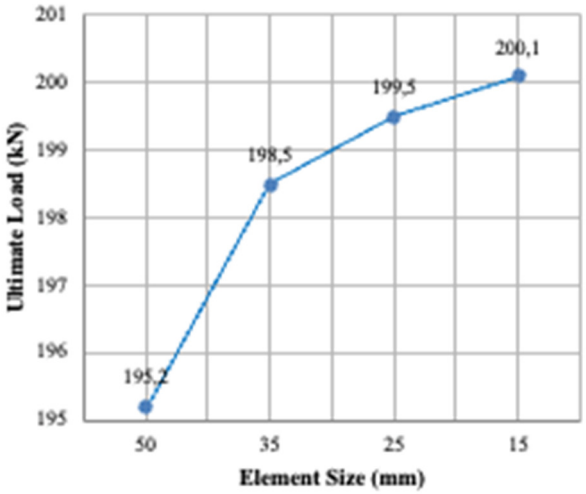

Fig. 3. Mesh convergence.

E. Analysis Outputs

In this study, the flexural performance of both the flat slab and beam-slab systems was evaluated through several structural response parameters. These included the crack pattern and propagation**,** which were observed based on the distribution of principal tensile strains within the concrete elements. The stress distribution in the reinforcement bars was also analyzed to assess the load transfer efficiency and the location of peak stresses under maximum loading conditions. Furthermore, the load-deflection behavior was recorded to understand the system's stiffness and deformation characteristics, with a particular focus on the maximum vertical displacement at mid-span**,** which represents the most critical region under flexural bending. Finally, the ultimate load-bearing capacity of each system was identified as the point at which the structure exhibited numerical instability or reached 90% material damage, marking the structural failure threshold in the simulation.

F. Assumptions and Limitations

Several assumptions and limitations were considered in this study to simplify the numerical modeling and ensure computational feasibility. It was assumed that both floor systems behave monolithically, with a perfect bond between the concrete and the reinforcing steel, meaning that there is no slip or separation during loading. The analysis did not account for time-dependent effects, such as creep, shrinkage, or temperature variations, which could influence long-term deflection and cracking behavior. Furthermore, while the finite element models were carefully constructed and calibrated using standard material properties, the results remain numerical in nature and were not experimentally validated within the scope of this study. However, references to established literature were used to verify the general accuracy and trends of the results.

III. RESULTS AND DISCUSSION

This research generated important numerical data on the flexural behavior of flat slab and beam-slab systems using FEM simulation in ABAQUS. The parameters analyzed were crack distribution, reinforcement stress, and maximum deflection.

A. Flat Slab System

- Cracks initiated at mid-span due to tensile stress exceeding the concrete's tensile capacity. At a load of 199.713 kN, the slab reached 90% damage, and the simulation terminated with an error, as portrayed in Figure 4.

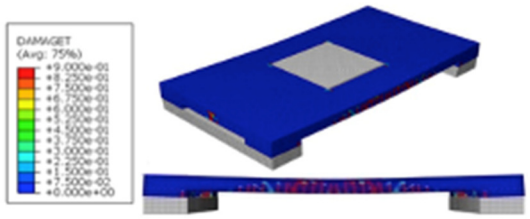

Fig. 4. Crack damage in the flat slab system.

- With a designed reinforcement grade of f_y = 493 MPa and f_u = 750 MPa, and under a peak load of 199.713 kN, the yield stress in the reinforcement reached 324 MPa at the supports and 517 MPa at mid-span, as illustrated in Figure 5.

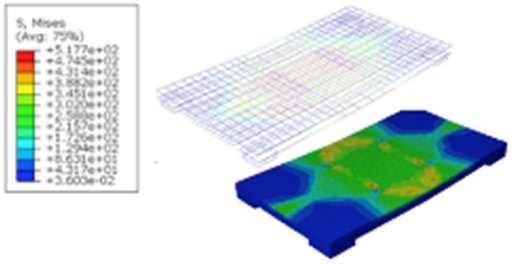

Fig. 5. Reinforcement ratio in the flat slab system.

The greatest deflection occurred at mid-span and was proportional to the increase in applied load. In the flat slab system, deflection was significantly influenced by the magnitude of the applied load. In the simulation using Abaqus, a load of 199.71 kN resulted in a maximum deflection of 16.12 mm at the center of the slab, as presented in Figure 6.

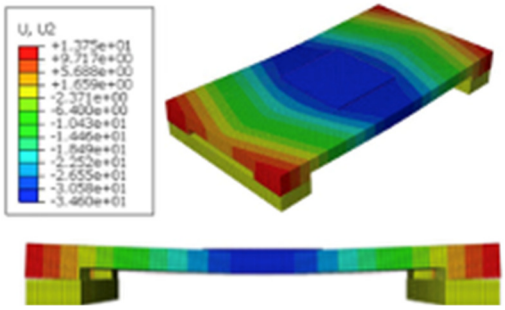

Fig. 6. Deflection in the flat slab system.

B. Beam-Slab System

- Initial cracking occurred in the bottom mid-span region due to tensile stresses exceeding the concrete's tensile capacity. The crack pattern propagated from the mid-span toward the supports because of both positive and negative bending moments. Under overloading conditions, cracks developed from the bottom tensile fibers at mid-span and from the top tensile fibers at the supports. At a load of 213.53 kN, the slab experienced 90% structural damage, and the simulation terminated with an error, as shown in Figure 7.

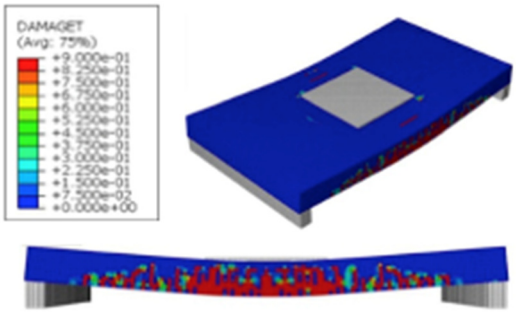

Fig. 7. Crack damage in the beam-slab system.

- The reinforcement ratio was designed using steel with a yield strength (f_y) of 493 MPa and an ultimate strength (f_u) of 750 MPa. Under a peak load of 213.53 kN, the reinforcement experienced a yield stress of 331 MPa at the support regions and 572 MPa at mid-span, as displayed in Figure 8.

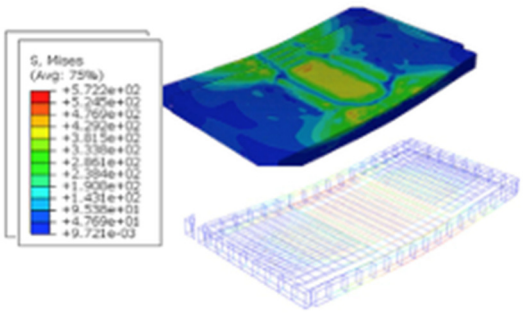

Fig. 8. Reinforcement ratio in the beam-slab system.

The maximum deflection occurred at mid-span and increased proportionally with the applied load. In the beam-slab system, deflection was significantly influenced by the magnitude of the applied load. In the ABAQUS simulation, a load of 213.53 kN resulted in a maximum deflection of 16.12 mm at the center of the slab, as illustrated in Figure 9.

C. Summary Comparison

1) Crack Pattern

In the flat slab system, cracks were distributed uniformly across the slab surface in a relatively random pattern. This behavior was mainly triggered by the applied concentrated load. Cracks formed at lower load levels than in the beam-slab system, indicating the flat slab's susceptibility to localized

stress concentrations due to the absence of structural confinement provided by beams. In contrast, the beam-slab system showed a more controlled and localized cracking pattern. Cracks were primarily concentrated around the support regions and at the slab-beam intersections. The beams played a significant role in limiting crack propagation by redistributing the applied forces, resulting in a more stable and confined cracking behavior compared with the flat slab system.

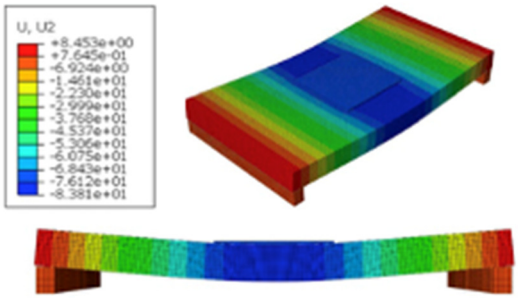

Fig. 9. Deflection in the beam-slab system.

2) Reinforcement Stress

The flat slab system experienced relatively lower stress on the reinforcement, especially in the mid-span area of the slab. This stress reduction can be attributed to the load being distributed evenly through a steel bearing plate, which helped spread the applied force across a wider area of the slab. On the other hand, the beam-slab system showed a significantly higher stress concentration, particularly within the beam regions. The bottom fibers of the beams were subjected to the most substantial tensile stress due to flexural action. In the slab portion itself, the stress was higher compared to the flat slab system. This increase was a result of the combined action between the slab and the supporting beams, which altered the distribution and magnitude of internal forces. This interaction produced higher localized stresses in critical regions, highlighting the influence of beam confinement on overall stress behavior.

3) Displacement (Deflection)

Regarding deflection, the flat slab system demonstrated smaller vertical displacements. The maximum deflection occurred at the mid-span of the slab, where the applied load was most concentrated. The system reached its ultimate capacity at a load of 199.71 kN, after which the simulation terminated due to excessive deformation and numerical instability. This indicates a lower flexural capacity but a stiffer initial response. In comparison, the beam-slab system experienced greater vertical displacement under loading. Like the flat slab, the maximum deflection also occurred at mid-span. However, this system withstood a higher load of up to 213.53 kN before the simulation failed. While the increased load capacity signifies improved flexural strength, the larger deflection reflects a more flexible structural response and suggests a trade-off between strength and stiffness.

4) Load-Deflection Comparison

To provide a clearer understanding of the flexural performance between the two systems, the load–deflection behavior was analyzed based on simulation results from ABAQUS. The deflection was measured at the mid-span of each slab system, representing the most critical location under bending loads. As illustrated in Figure 10, the flat slab system exhibited a stiffer response, reaching its ultimate load of 199.71 kN at a deflection of 16.12 mm. In contrast, the beam-slab system demonstrated greater flexibility, sustaining a higher ultimate load of 213.53 kN with a larger deflection of 39.35 mm. These results indicate a trade-off between flexural stiffness and load-carrying capacity. The presence of beams in the beam-slab system enhanced the flexural capacity but exhibited greater deformation under loading due to the lower overall flexural stiffness of the flat slab system compared to the beam-slab system. This increased deflection remained within serviceability limits and reflected the inherent flexibility of the flat slab configuration rather than structural inadequacy.

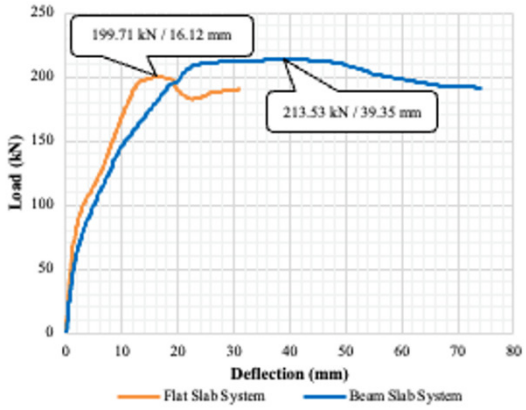

Fig. 10. Comparison of load–deflection curves.

As summarized in Table I, the flat slab system demonstrated a stiffer response with a higher stiffness ratio of 12.39 kN/mm, sustaining an ultimate load of 199.71 kN at a deflection of only 16.12 mm. In contrast, the beam-slab system exhibited greater flexibility, reaching a higher ultimate load of 213.53 kN but with a much larger deflection of 39.35 mm, corresponding to a lower stiffness ratio of 5.43 kN/mm. These results highlight a clear trade-off between flexural stiffness and load-carrying capacity, where the flat slab provides better serviceability in terms of deformation control, while the beam-slab system offers enhanced strength capacity.

In addition to strength assessment, serviceability was evaluated by comparing the maximum deflections with the code limits specified in [17, 18, 7], which propose deflection limits of L/250 for the total load and L/500 for the live load. The short-term deflections of both slab systems remained within these limits, indicating sufficient stiffness under service conditions. Long-term effects due to creep and shrinkage were estimated using the effective modulus method with a creep coefficient of 2, resulting in long-term deflections approximately 2.1–2.3 times greater than the short-term values. Even with these increases, both the flat slab and beam-slab systems continued to satisfy serviceability requirements, confirming satisfactory long-term performance. These results also align well with experimental and numerical studies on RC slabs. For example, authors in [32] reported that flat slabs

typically exhibit lower ultimate load capacity but smaller service deflections compared with beam-slab systems, consistent with the present findings, where the flat slab reached 199.71 kN at 16.12 mm deflection, while the beam-slab sustained 213.53 kN at 39.35 mm. Likewise, authors in [15] found that slabs supported by beams achieve higher load-carrying capacity but experience larger deflections under ultimate loading, mirroring the trade-off observed in this study. Additionally, authors in [26] demonstrated through FEM-based cost-efficiency analyses that increasing flat-slab stiffness improves deformation control but slightly reduces ultimate capacity. These parallels confirm that the numerical results obtained in this study are consistent with established trends in the literature. The unique contribution of this work lies in maintaining identical reinforcement weight and concrete volume for both systems, enabling a more balanced and equitable comparison. Based on the numerical results and supporting literature, a decision-making guideline for selecting between flat slab and beam-slab systems is proposed and summarized in Figure 11.

TABLE I. COMPARATIVE PERFORMANCE OF FLAT SLAB AND BEAM-SLAB SYSTEMS

Parameter	Flat slab system	Beam-slab system	Difference (beam-slab versus flat slab)	Remarks
Ultimate load (kN)	199.71	213.53	+6.9%	Beam-slab sustains higher load capacity
Maximum deflection (mm)	16.12	39.35	+144%	Flat slab is stiffer; beam-slab is more flexible
Stiffness ratio (kN/mm)	12.39	5.43	Flat slab ≈ 128% stiffer	Flat slab provides greater resistance to deformation
Structural performance	Balanced stiffness	Greater load capacity	–	Indicates a trade-off between stiffness and strength

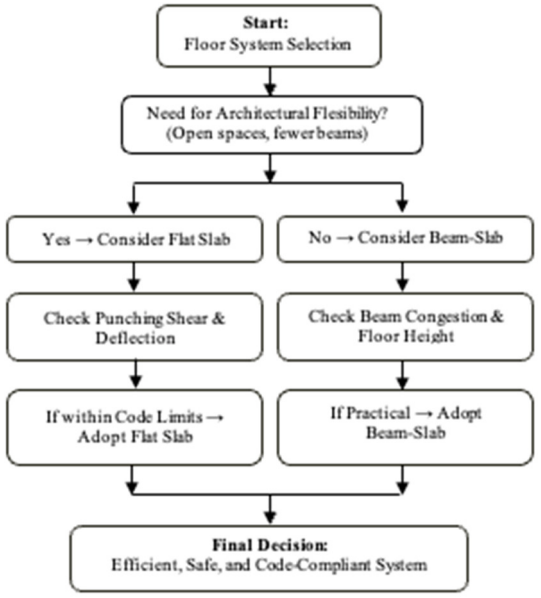

Fig. 11. Flowchart for selecting flat slab versus beam-slab systems.

IV. CONCLUSIONS

A. Conclusion

This study performed a numerical comparison between flat slab and beam-slab systems using ABAQUS under controlled conditions of identical concrete volume (0.51 m³) and reinforcement weight (57.44 kg). The main outcomes are:

- The flat slab system exhibited earlier crack initiation and a lower ultimate capacity (199.71 kN, deflection 16.12 mm) yet showed a relatively stiff response and uniform crack distribution. These characteristics make it advantageous in applications prioritizing architectural flexibility and construction simplicity.
- The beam-slab system reached a higher load capacity (213.53 kN) with improved crack control near supports, but deflected more significantly (39.35 mm). This indicates that the presence of beams enhances load redistribution and flexural strength, though, at the cost of greater deformation and construction complexity.
- The stress analysis showed that reinforcement stresses were more highly concentrated in the beam-slab joints, while the flat slab exhibited a more uniform stress distribution.

The novelty of this study lies in its controlled comparison using identical material quantities, addressing a methodological gap seldom explored in previous research. By isolating the influence of structural configuration, the results reveal the inherent trade-offs between strength, serviceability, and constructability. This provides a practical benchmark for engineers when selecting slab systems based on project priorities such as span requirements, ceiling height constraints, and construction efficiency.

B. Recommendations

- Future work should include experimental validation of the numerical findings, particularly for cracking and deflection profiles to strengthen design reliability.
- Extending the analysis to incorporate serviceability criteria (ACI/Eurocode deflection limits, long-term creep and shrinkage) will enhance practical applicability.
- Broader parametric studies considering reinforcement ratios, drop panel dimensions, and seismic effects are encouraged to support design optimization and code development for both slab systems.

ACKNOWLEDGMENT

This research was funded by the Ministry of Higher Education, Science, and Technology of the Republic of Indonesia through the 2025 Fiscal Year Kemdiktisaintek Research Grant Program under the Postgraduate Program Scheme – Master's Thesis Research (PPS-PTM), with contract number LPPM Unhas: 02209/UN4.22/PT.01.03/2025. The authors gratefully acknowledge this support.

REFERENCES

[1] G. M. Werdina, "Finite Element Analysis of Fiber Reinforced Concrete Slabs under Torsion," *The Open Civil Engineering Journal*, vol. 18, Oct. 2024, https://doi.org/10.2174/0118741495354199241001110433.

[2] M. Shokri, M. Edalati, S. M. Mirhosseini, and E. Zeighami, "FE Analysis on Size Effect in Torsional Behavior of Rectangular RC Beams with and Without FRP Strengthening," *KSCE Journal of Civil Engineering*, vol. 28, no. 5, pp. 1836–1852, May 2024, https://doi.org/10.1007/s12205-024-0020-0.

[3] A. Ghali, R. Favre, and M. Elbadry, *Concrete Structures: Stresses and Deformations: Analysis and Design for Serviceability, Third Edition*, 3rd ed. London: CRC Press, 2018.

[4] I. A. Attallah, "Finite Element Modelling and Parametric Analysis of High Strength Thin Reinforced Concrete Slabs Strengthened by CFRP Laminates," *ERJ. Engineering Research Journal*, vol. 46, no. 1, pp. 89–98, Jan. 2023, https://doi.org/10.21608/erjm.2022.161289.1209.

[5] O. C. Zienkiewicz and R. L. Taylor, *The Finite Element Method: Its Basis and Fundamentals*. Butterworth-Heinemann, 2013.

[6] R. Al-Rousan and B. R. Alnemrawi, "NLFEA of the Behavior of Polypropylene-Fiber-Reinforced Concrete Slabs with Square Opening," *Buildings*, vol. 14, no. 2, Feb. 2024, Art. no. 480, https://doi.org/10.3390/buildings14020480.

[7] A. W. Beeby and R. S. Narayanan, *Designers' Guide to EN 1992-1-1 Eurocode 2: Design of Concrete Structures: General Rules and Rules for Buildings and Structural Fire Design*. Thomas Telford, 2005.

[8] H. Ahmad, A. Elnemr, N. Ali, Q. Hussain, K. Chaiyasarn, and P. Joyklad, "Finite Element Analysis of Glass Fiber-Reinforced Polymer-(GFRP) Reinforced Continuous Concrete Beams," *Polymers*, vol. 13, no. 24, Jan. 2021, Art. no. 4468, https://doi.org/10.3390/polym13244468.

[9] I. Edri and D. Yankelevsky, "Numerical framework for assessing punching shear behavior in integrity-reinforced concrete flat slab specimens," *Structures*, 2025, https://doi.org/10.1016/j.istruc.2025.108823.

[10] A. Qsymah and M. Ayasrah, "Finite Element Analysis of Two-Way Reinforced Concrete Slabs Strengthened with FRP Under Flexural Loading," *Buildings*, vol. 14, no. 11, Nov. 2024, Art. no. 3389, https://doi.org/10.3390/buildings14113389.

[11] A. N. Ameen and M. H. Al-Sherrawi, "Structural Behavior of Reinforced Concrete Flat Plates Strengthened by Horizontal Reinforcement," *Engineering, Technology & Applied Science Research*, vol. 14, no. 4, pp. 15305–15311, Aug. 2024, https://doi.org/10.48084/etasr.7261.

[12] A. Kutsenko and O. Kutsenko, "Effect of reinforcement on the crack resistance of concrete slabs," *Machinery & Energetics*, vol. 3, no. 13, pp. 34–42, Aug. 2022, https://doi.org/10.31548/machenergy.13(3).2022.34-42.

[13] B. N. Moraes Neto, J. A. O. Barros, and G. S. S. A. Melo, "A model for the prediction of the punching resistance of steel fibre reinforced concrete slabs centrically loaded," *Construction and Building Materials*, vol. 46, pp. 211–223, Sept. 2013, https://doi.org/10.1016/j.conbuildmat.2013.04.034.

[14] G. Zani, P. Martinelli, and M. di Prisco, "Role of the tensile constitutive modeling on the structural response of fiber reinforced concrete flat slabs: A numerical study," *Structural Concrete*, vol. 24, no. 1, pp. 1313–1327, 2023, https://doi.org/10.1002/suco.202200186.

[15] F. Stochino and F. Lopez Gayarre, "Reinforced Concrete Slab Optimization with Simulated Annealing," *Applied Sciences*, vol. 9, no. 15, Jan. 2019, Art. no. 3161, https://doi.org/10.3390/app9153161.

[16] E. M. Mouwainea and A. M. I. Said, "Numerical Modeling of Reinforced Concrete Slabs under Impact Loading," *Key Engineering Materials*, vol. 857, pp. 99–108, Aug. 2020, https://doi.org/10.4028/www.scientific.net/KEM.857.99.

[17] *ACI 318-19 Building Code Requirements for Structural Concrete*. USA: American Concrete Institute, 2019.

[18] B. S. Institution, *Eurocode 2: Design of Concrete Structures : Part 1-1: General Rules and Rules for Buildings*. British Standards Institution, 2004.

[19] "ABAQUS Documentation," *Dassault Systèmes*, Aug. 24, 2023. https://www.3ds.com/support/documentation.

[20] *Model Code 2010 Final draft*. CEB-FIB, 2012.

[21] P. M. Lewiński and P. P. Więch, "Finite element model and test results for punching shear failure of RC slabs," *Archives of Civil and Mechanical Engineering*, vol. 20, no. 2, Mar. 2020, Art. no. 36, https://doi.org/10.1007/s43452-020-00037-x.

[22] E. El-Salakawy, K. Soudki, and M. A. Polak, "Punching Shear Behavior of Flat Slabs Strengthened with Fiber Reinforced Polymer Laminates," *Journal of Composites for Construction*, vol. 8, no. 5, pp. 384–392, Oct. 2004, https://doi.org/10.1061/(ASCE)1090-0268(2004)8:5(384).

[23] M. Q. Abdul Sahib, R. Aghayari, M. J. Moradi, and M. Tahamouli Roudsari, "Experimental Investigation on the Rehabilitation of RC Flat Slabs Using CFRP Sheets to Enhance Punching Shear Capacity," *Buildings*, vol. 14, no. 1, Jan. 2024, Art. no. 153, https://doi.org/10.3390/buildings14010153.

[24] M. H. Meisami, D. Mostofinejad, and H. Nakamura, "Strengthening of flat slabs with FRP fan for punching shear," *Composite Structures*, vol. 119, pp. 305–314, Jan. 2015, https://doi.org/10.1016/j.compstruct.2014.08.041.

[25] B. Al-Atta, R. Kalfat, and R. Al-Mahaidi, "Numerical investigation into RC slabs strengthened using FRP and hybrid anchors," *Structures*, vol. 58, Dec. 2023, Art. no. 105558, https://doi.org/10.1016/j.istruc.2023.105558.

[26] M. A. Adam, A. M. Erfan, F. A. Habib, and T. A. El-Sayed, "Structural Behavior of High-Strength Concrete Slabs Reinforced with GFRP Bars," *Polymers*, vol. 13, no. 17, Sept. 2021, Art. no. 2997, https://doi.org/10.3390/polym13172997.

[27] C. Paknahad, M. Tohidi, A. Bahadori-Jahromi, and S. Room, "A Comparative Study of Optimised Embodied Carbon and Cost in RC Slab Structures," *Sustainability*, vol. 17, no. 19, Jan. 2025, Art. no. 8662, https://doi.org/10.3390/su17198662.

[28] E. Rizk, H. Marzouk, A. Hussein, and M. Hossin, "Effect of reinforcement ratio on punching capacity of RC plates," *Canadian Journal of Civil Engineering*, vol. 38, no. 7, pp. 729–740, 2011, https://doi.org/doi:10.1139/L11-053.

[29] Y. Jia and J. C. L. Chiang, "Finite Element Analysis of Punching Shear of Reinforced Concrete Slab–Column Connections with Shear Reinforcement," *Applied Sciences*, vol. 12, no. 19, Jan. 2022, Art. no. 9584, https://doi.org/10.3390/app12199584.

[30] C. Yusnar, "Punching Shear Behavior on High Strength Concrete," *IOP Conference Series: Materials Science and Engineering*, vol. 536, no. 1, Mar. 2019, Art. no. 012115, https://doi.org/10.1088/1757-899X/536/1/012115.

[31] D. Mostofinejad, N. Jafarian, A. Naderi, A. Mostofinejad, and M. Salehi, "Effects of openings on the punching shear strength of reinforced concrete slabs," *Structures*, vol. 25, pp. 760–773, June 2020, https://doi.org/10.1016/j.istruc.2020.03.061.

[32] H. H. Ghayeb, R. S. Atea, M. A.-A. Al-Kannoon, F. W. Lee, L. S. Wong, and K. H. Mo, "Performance of reinforced concrete flat slab strengthened with CFRP for punching shear," *Case Studies in Construction Materials*, vol. 18, July 2023, Art. no. e01801, https://doi.org/10.1016/j.cscm.2022.e01801.

[33] C. Zou, Z. Ibrahim, H. Hashim, A. Jamadin, and P. Ayough, "Nonlinear analysis of reinforced concrete slabs under high-cyclic fatigue loading," *Journal of Materials Research and Technology*, vol. 21, pp. 992–1012, Nov. 2022, https://doi.org/10.1016/j.jmrt.2022.09.091.

[34] A. Al-Ateyat, S. Barakat, M. T. Junaid, S. Altoubat, M. Maalej, and R. Awad, "Experimental and Numerical Analysis of Punching Shear of GFRP-RC Slabs," *Civil Engineering Journal*, vol. 10, pp. 344–358, Jan. 2025, https://doi.org/10.28991/CEJ-SP2024-010-017.

[35] Y. Almomani, R. Alawadi, A. Tarawneh, A. Alghossoon, and A. Aldiabat, "Punching Shear of FRP-RC Slab–Column Connections: A Comprehensive Database," *Journal of Composites Science*, vol. 8, no. 4, Apr. 2024, Art. no. 145, https://doi.org/10.3390/jcs8040145.

[36] X. Teng and Y. X. Zhang, "Nonlinear Finite Element Analyses of FRP-Strengthened Concrete Slabs under Fixed-Point Cyclic Loading," *Journal of Composites for Construction*, vol. 19, no. 3, June 2015, Art. no. 04014057, https://doi.org/10.1061/(ASCE)CC.1943-5614.0000519.

[37] J. Joseph, N. Nasruddin, and H. Hartawan, "Comparative Analysis of Flexural Strength and Reinforcement Weight of Flat Slab Floor System

and Beam-Slab Floor System," *International Journal of Computational and Experimental Science and Engineering*, vol. 11, no. 2, Apr. 2025, https://doi.org/10.22399/ijcesen.1590.

[38] H. Sisay and T. Wondimu, "A Parametric Study on Lateral Load Behavior of Interior Flat Plate - Column Connections," *ASEAN Engineering Journal*, vol. 12, no. 2, pp. 91–100, June 2022, https://doi.org/10.11113/aej.v12.17107.

[39] A. Y. M, S. Prashanth, P. Pandit, G. M. G, and A. Shetty, "Finite Element Analysis of Bond Behavior in Corroded Reinforced Concrete Beams: State-of-the-Art," *Journal of Applied Engineering Science*, vol. 21, no. 4, pp. 1031–1042, Nov. 2023, https://doi.org/10.5937/jaes0-42252.

[40] *ACI 421.1R-20 - Guide To Shear Reinforcement For Slabs*. USA: American Concrete Institute, 2020.